Fig. 3. The validation of representative altered splicing events in TDP-43-silenced primary cortical neurons and FUS-silenced primary cortical neurons. Eight exons with differential expression in both TDP-43-silenced neurons and FUS-silenced neurons were validated by semiquantitative RT-PCR. The top panel provides a schematic of splicing changes mediated by TDP-43 and/or FUS. The second and third panels display representative RT-PCR results for the indicated exons and the densitometric quantification (ratio of inclusion to exclusion) of these results ($n = 3$; mean and SD) after either TDP-43 or FUS depletion. *$p < 0.05$ by t-test. Statistics were done by one-way ANOVA and Tukey test. * ($p < 0.05$), ** ($p < 0.01$), and *** ($p < 0.001$) denote significant differences.

Table 1
Gene Ontology terms for gene expression/alternative splicing in TDP-43- or FUS-silenced neurons.

shTDP-43	Gene expression		shFUS	Gene expression	
GO ID	Term	*p*-Value	GO ID	Term	*p*-Value
GO:0007264	Small GTPase mediated signal transduction	8.37E−07	GO:0019637	Organophosphate metabolic process	3.68E−04
GO:0007242	Intracellular signaling cascade	1.04E−05	GO:0006644	Phospholipid metabolic process	4.89E−04
GO:0044271	Nitrogen compound biosynthetic process	2.98E−04	GO:0016055	Wnt receptor signaling pathway	5.21E−04
GO:0006790	Sulfur metabolic process	9.94E−04	GO:0009100	Glycoprotein metabolic process	5.30E−04
GO:0009100	Glycoprotein metabolic process	0.00169596	GO:0007264	Small GTPase mediated signal transduction	5.91E−04
GO:0009101	Glycoprotein biosynthetic process	0.0019038	GO:0006650	Glycerophospholipid metabolic process	8.42E−04
GO:0018130	Heterocycle biosynthetic process	0.0033067	GO:0007242	Intracellular signaling cascade	0.00122745
GO:0022604	Regulation of cell morphogenesis	0.00426464	GO:0007265	Ras protein signal transduction	0.00389788
GO:0016055	Wnt receptor signaling pathway	0.00455985	GO:0046486	Glycerolipid metabolic process	0.00481341
GO:0031344	Regulation of cell projection organization	0.00619132	GO:0006665	Sphingolipid metabolic process	0.00514754
GO:0043085	Positive regulation of catalytic activity	0.0063261	GO:0030384	Phosphoinositide metabolic process	0.00562443
GO:0031345	Negative regulation of cell projection organization	0.00656187	GO:0006793	Phosphorus metabolic process	0.00563812
GO:0043413	Biopolymer glycosylation	0.00855583	GO:0006796	Phosphate metabolic process	0.00563812
GO:0006486	Protein amino acid glycosylation	0.00855583	GO:0006643	Membrane lipid metabolic process	0.00613362
GO:0070085	Glycosylation	0.00855583	GO:0009101	Glycoprotein biosynthetic process	0.00691847
GO:0010975	Regulation of neuron projection development	0.00912726	GO:0051348	Negative regulation of transferase activity	0.00924863
GO:0030384	Phosphoinositide metabolic process	0.010632	GO:0006600	Creatine metabolic process	0.01095567
GO:0010769	Regulation of cell morphogenesis involved in differentiation	0.01225994	GO:0044242	Cellular lipid catabolic process	0.01200742
GO:0019932	Second-messenger-mediated signaling	0.01617062	GO:0006486	Protein amino acid glycosylation	0.01276803
GO:0050770	Regulation of axonogenesis	0.01657312	GO:0070085	Glycosylation	0.01276803

shTDP-43	Alternative splicing		shFUS	Alternative splicing	
GO ID	Term	*p*-Value	GO ID	Term	*p*-Value
GO:0016192	Vesicle-mediated transport	2.76E−05	GO:0045202	Synapse	6.85E−07
GO:0044057	Regulation of system process	2.41E−04	GO:0042995	Cell projection	2.54E−06
GO:0006936	Muscle contraction	5.09E−04	GO:0043005	Neuron projection	2.29E−05
GO:0003012	Muscle system process	7.75E−04	GO:0005856	Cytoskeleton	1.73E−04
GO:0006897	Endocytosis	0.00107681	GO:0005886	Plasma membrane	1.88E−04
GO:0010324	Membrane invagination	0.00107681	GO:0043232	Intracellular non-membrane-bounded organelle	2.07E−04
GO:0046903	Secretion	0.00244805	GO:0043228	Non-membrane-bounded organelle	2.07E−04
GO:0048167	Regulation of synaptic plasticity	0.00322575	GO:0044456	Synapse part	3.76E−04
GO:0050804	Regulation of synaptic transmission	0.00339707	GO:0030424	Axon	5.70E−04
GO:0050808	Synapse organization	0.00342093	GO:0031252	Cell leading edge	7.01E−04
GO:0043524	Negative regulation of neuron apoptosis	0.0036232	GO:0044463	Cell projection part	7.08E−04
GO:0051969	Regulation of transmission of nerve impulse	0.00432752	GO:0030054	Cell junction	7.20E−04
GO:0006887	Exocytosis	0.00477415	GO:0015630	Microtubule cytoskeleton	0.00738251
GO:0031644	Regulation of neurological system process	0.00525083	GO:0045211	Postsynaptic membrane	0.00825557
GO:0032940	Secretion by cell	0.00587779	GO:0042734	Presynaptic membrane	0.0133955
GO:0006816	Calcium ion transport	0.00667547	GO:0044430	Cytoskeletal part	0.02340953
GO:0016044	Membrane organization	0.0067241	GO:0044459	Plasma membrane part	0.02454379
GO:0046777	Protein amino acid autophosphorylation	0.00788146	GO:0001726	Ruffle	0.03547283
GO:0007628	Adult walking behavior	0.01199082	GO:0032589	Neuron projection membrane	0.04340658
GO:0043523	Regulation of neuron apoptosis	0.01330492	GO:0005938	Cell cortex	0.04544057

The relative quantity of each transcript was calculated by creating a standard curve using the cycle thresholds for serial dilutions of complementary DNA (cDNA) samples, normalized to quantities of β-actin. The PCR was performed in triplicate for each sample, and all experiments were repeated twice. iQ SYBR Green Supermix (BioRad) and the sets of primers listed in Supplementary Table 1 were used for real-time quantitative polymerase chain reaction (qPCR) amplifications.

Table 2
Differentially expressed genes regulated by both TDP-43 and FUS.

Gene symbol	Gene name	shTDP_FC	shFUS_FC
Tgfbr1	Transforming growth factor, beta receptor 1	0.38	0.40
Tap1	Transporter 1, ATP-binding cassette, sub-family B (MDR/TAP)	0.53	0.41
Ccbe1	Collagen and calcium binding EGF domains 1	0.60	0.60
Sla	src-like adaptor	0.61	0.58
Vamp1	Vesicle-associated membrane protein 1	0.66	0.64
Rab15	RAB15, member RAS oncogene family	1.96	2.10
Taf9b	TAF9B RNA polymerase II, TATA box binding protein (TBP)-associated factor	2.00	3.13
Ilk	Integrin-linked kinase	2.08	2.16
Nacc1	Nucleus accumbens associated 1, BEN and BTB (POZ) domain containing	2.29	2.49
Qpctl	Glutaminyl-peptide cyclotransferase-like	2.37	2.63
Syt17	Synaptotagmin 17	3.08	1.82
Stx1a	Syntaxin 1A	3.08	2.45

Table 3
Genes with altered exon splicing regulated by both TDP-43 and FUS.

Gene symbol	Gene name	Spliced site	
Braf	Braf transforming gene	Exon12	Skipping
Camk2a	Calcium/calmodulin-dependent protein kinase II alpha	Exon14	Skipping
Cttn	Cortactin	Exon11	Skipping
Deaf1	Deformed epidermal autoregulatory factor 1	Exon2	Skipping
Erc2	ELKS/RAB6-interacting/CAST family member 2	Exon12	Skipping
Kcnip1	Kv channel-interacting protein 1	Exon2	Skipping
Ncor1	Nuclear receptor corepressor 1	Exon9	Skipping
Anks1b	Ankyrin repeat and sterile alpha motif domain containing 1B	Exon7	Inclusion

3. Results

3.1. The shRNA-mediated silencing of TDP-43 and FUS in primary cortical neurons using lentivirus

To compare the global profiles of RNA molecules regulated by TDP-43 and FUS in primary cortical neurons, we produced TDP-43-silenced primary motor neurons by infecting neurons with lentivirus expressing shRNA against TDP-43; control neurons were produced by infection with lentivirus expressing RNA against a scrambled control. The profiles of FUS-silenced primary cortical neurons using shFUS1 and shFUS2 were established in a previous study [26]. The purity of the primary cortical neurons was confirmed through immunostaining. We successfully established the desired primary cortical neurons with a purity of greater than 95% (Supplementary Fig. S1A).

The expression levels of TDP-43 were suppressed by approximately 60–90% by shTDP1 or shTDP2, as measured by real-time qPCR (Supplementary Fig. S1B). The expression levels of FUS were also suppressed by 80–90% by shFUS1 or shFUS2, as reported previously [26]. The protein levels of TDP-43 were markedly lower in primary neurons infected with shTDP1 and shTDP2 than in neurons infected with the shCont based on the immunoblot analysis (Supplementary Fig. S1C, left). In addition, a reduction in FUS protein levels was observed in primary neurons infected with shFUS1 or shFUS2 (Supplementary Fig. S1C, right).

As a control for the RNA-binding protein-silencing model, we knocked down the Cugbp1 gene in primary cortical neurons and confirmed that this knockdown produced a silencing efficiency of greater than 70% (Supplementary Fig. S2).

3.2. Significant overlap in the transcriptomes of TDP-43-silenced neurons and FUS-silenced neurons

We analyzed gene expression levels and alternative splicing in TDP-43-silenced primary neurons using the Affymetrix GeneChip Mouse Exon 1.0 ST Array (GEO Accession No. GSE46148). We used Student's t-test to compare the gene-level signal intensities of three controls treated with shCont with the gene-level signal intensities of three samples treated with either shTDP1 or shTDP2. Among the 21,603 genes on the mouse exon array, 1411 genes had p-values ≤ 0.01 for both shTDP1 and shTDP2 treatments in the t-tests, and the correlation coefficient between the fold changes of the shTDP1 and shTDP2 treatments was 0.83 (Supplementary Fig. S3A).

We also analyzed alternative splicing profiles by filtering the exon-level signal intensities using a threshold of a t-test p-value ≤ 0.1. This filtering yielded 4973 exons that were altered by both shTDP1 and shTDP2, with a correlation coefficient of 0.801 (Supplementary Fig. S3B). To identify common effects produced by silencing TDP-43 and silencing FUS, we compiled a list of differentially expressed genes and alternatively spliced exons in primary cortical neurons silenced by shTDP-43 and in primary cortical neurons silenced by shFUS. By applying the threshold of a t-test p-value of ≤ 0.05 and a fold change of ≤ 0.67 or ≥ 1.5 for both shTDP1 and shTDP2, we obtained 204 genes with altered expression levels upon TDP-43 knockdown. Similarly, 183 genes were obtained for FUS by applying the threshold of a t-test p-value of ≤ 0.05 and a fold change value of ≤ 0.67 or ≥ 1.5 for both shFUS-1 and shFUS-2. Venn diagrams indicated that the set of genes or exons with expression that were differentially and consistently regulated by FUS markedly overlapped with the corresponding set of genes or exons for TDP-43 (t-test, $p < 0.05$). In particular, an overlap

of more than 25% was observed among the gene expression profiles of shTDP-43- and shFUS-treated neurons (Fig. 1A, top panel; 51/204 (25.0%) of the genes for shTDP-43; 51/183 (27.9%) of the genes for shFUS).

We also filtered the exon-level signal intensities by applying a threshold of a t-test p-value of ≤ 0.05 and a fold change value of ≤ 0.67 or ≥ 1.5. We then determined TDP-43- and FUS-regulated exons as well as the overlap between these exons using the same approach that we applied for gene expression. We obtained 675 TDP-43-regulated genes and 429 FUS-regulated genes with altered exon expression. Venn diagrams indicate that there was an overlap of approximately 10% between the alternative splicing profiles produced by shFUS and the alternative splicing profiles produced by shTDP-43 (Fig. 1A, bottom panel; 61/674 (9.1%) of the genes for shTDP-43; 61/428 (14.3%) of the genes for shFUS).

We then compared the changes in the overlapping genes or exons affected by both shTDP-43 and shFUS after filtering these genes and exons using a t-test (with a threshold of $p < 0.1$). The fold change plot analysis demonstrated a strong correlation between shTDP-43 and shFUS with respect to gene expression (Fig. 1B left; $R^2 = 0.78$); in contrast, the gene expression profile for neurons transduced with shRNA targeting a different RNA-binding protein, Cugbp1, did not correlate well with the expression profiles of neurons transduced with shTDP-43 ($R^2 = 0.46$) or shFUS ($R^2 = 0.53$) (Supplementary Fig. S4A). The fold change plot analysis of exon splicing also demonstrated a moderate correlation between shTDP-43 and shFUS (Fig. 1B right; $R^2 = 0.64$). The exon splicing profile for neurons silenced with shRNA against Cugbp1 showed lesser correlation with the exon splicing profiles of neurons transduced with shTDP-43 ($R^2 = 0.52$) or shFUS ($R^2 = 0.48$) (Supplementary Fig. S4B).

We next analyzed the Gene Ontology (GO) terms for the genes that were regulated by TDP-43 and FUS (t-test, $p < 0.1$; fold change of ≤ 0.77 or ≥ 1.3) using the Database for Annotation, Visualization and Integrated Discovery (DAVID), version 6.7 [27,28]. Genes regulated by TDP-43 were mainly categorized as being involved in signaling cascades and metabolic processes, and the GO terms for these genes were similar to the GO terms for genes regulated by FUS. In the list of the top 20 GO terms for genes with TDP-43-regulated expression and the corresponding list for genes with FUS-regulated expression, we identified eight common GO terms, including "small GTPase-mediated signal transduction" and "Wnt receptor signaling pathway" (Table 1). We also compiled the list of top 20 GO terms for genes with Cugbp1-regulated expression (Supplementary Table S2). Only one and three common GO terms were identified in between the lists of Cugbp1- and TDP-43-regulated expression (GO:0007264) and Cugbp1- and FUS-regulated expression (GO:0007264, 0019637, and 0006644), respectively. In contrast, the GO terms for genes with TDP-43- or FUS-related alternative splicing regulation mainly referred to various neuronal functions; however, none of the same GO terms appeared in both the list of the top 20 GO terms for genes with TDP-43-regulated alternative splicing and the corresponding list for genes with FUS-regulated alternative splicing (Table 1).

3.3. Gene expression profiles are similar among the top 20 genes regulated by TDP-43 and FUS

We next investigated the detailed gene expression profiles of TDP-43-silenced primary cortical neurons. By filtering gene-level signal intensities using a t-test (with a threshold of p-value ≤ 0.1) and fold change (which was required to be ≤ 0.67 or ≥ 1.5), genes with differential expression in TDP-43-silenced primary cortical neurons were selected. Fourteen of the top 20 genes with expression regulated by TDP-43 were also regulated by FUS (Supplementary Table S3). To select genes with differential expression upon changes in FUS regulation, gene-level signal intensities in the profile of FUS-silenced primary

cortical neurons were filtered using a t-test (with a threshold of p-value ≤ 0.1) and fold change (which was required to be ≤ 0.67 or ≥ 1.5). Genes that were differentially expressed in both TDP-43-silenced primary cortical neurons and FUS-silenced primary cortical neurons (as determined by the p-value ≤ 0.1 and fold change of ≤ 0.67 or ≥ 1.5 requirements) are listed with their fold change values in Table 2. The list of commonly regulated genes includes 12 genes: five downregulated genes, such as *Tgfbr1* (transforming growth factor-β receptor I; Fig. 2A), and seven upregulated genes, such as *Stx1a* (syntaxin 1A; Fig. 2B). The results were validated using quantitative reverse transcription polymerase chain reaction (qRT-PCR) and shown as mRNA expression ratio to β-actin (Fig. 2) and Gapdh (Supplementary Fig. S5).

3.4. Genes with altered exon splicing regulated by both TDP-43 and FUS

After filtering the exons in genes that were differentially expressed in both shTDP1- and shTDP2-treated neurons, using the threshold of a t-test p-value of ≤ 0.1 and a fold change of ≥ 1.3 in primary neurons, we compared these exons with the profiles of alternatively spliced exons in shFUS1 and shFUS2 to obtain genes with altered splicing events that were commonly regulated by both TDP-43 and FUS. After validation by RT-PCR, we obtained 8 exons with alternative splicing events regulated by both TDP-43 and FUS (Table 3 and Fig. 3).

4. Discussion

Both TDP-43 and FUS are involved in multiple levels of RNA processing, and mutations in these two genes are responsible for familial ALS and FTLD. Although TDP-43 and FUS pathologies appear to largely be mutually exclusive, the molecular and functional similarities between these two molecules suggest that TDP-43 and FUS may share a common downstream pathway leading to neuronal degeneration [29,30].

Genes with altered expression levels or alternatively spliced exons in both TDP-43- and FUS-silenced primary neurons have fundamental functions in neurons, suggesting that transcriptome changes produced by loss-of-function mutations of TDP-43 and/or FUS may lead to neuronal cell death. This conjecture is supported by cross-rescue findings from fish and fly models in which FUS overexpression rescued the defect phenotype caused by TDP-43 knockout [20,21].

How do TDP-43 and FUS regulate common downstream genes and exons? These proteins do not appear to share the same binding target RNAs in neuronal tissue; in particular, it has been reported that the consensus sequences of TDP-43 are (UG) repeats [31,32], whereas FUS has a widespread RNA binding pattern [26,33]. Research has indicated that these two RNA binding proteins may target distinct sets of cytoplasmic mRNA molecules in NSC-34 cells [34]. Although we found that there was an overlap of approximately 10% between genes with altered splicing after shFUS treatment and genes with altered splicing after shTDP-43 treatment, the regulation mechanism of common alternative splicing events remains unclear.

Our results indicated that 25% of genes with altered gene expression levels and 10% of genes with alternatively spliced exons were common to the transcriptome profiles of both TDP-43-silenced primary cortical neurons and FUS-silenced primary cortical neurons. These findings were comparable to the results reported by Lagier-Tourenne et al., which demonstrated that in adult mouse striatum, there was an overlap of more than 10% between alternative splicing events observed due to TDP-43 knockdown and alternative splicing events observed due to FUS knockdown [35]. Discrepancies between this prior study and the current investigation with respect to targeted RNAs could reflect the different cell types used in these studies; we specifically assessed neurons, whereas the mouse striatum contains a variety of cells, including neurons, glial cells, and other cell types.

In fact, in a recent study, we found distinct FUS-regulated transcriptomes among different cell lineages [24].

Among the target RNA molecules that we identified, *Stx1A* is one of the most differentially upregulated genes in both TDP-43-silenced neurons and FUS-silenced neurons (Table 2). Stx1A encodes Syntaxin 1A, which is a member of the syntaxin super family that is associated with the vesicle fusion process as a component of the SNARE complex [36]. The overexpression of Stx1A disturbed synaptic vesicle exocytosis in hippocampal neurons [37], suggesting that up-regulation of Stx1A by silencing TDP-43 or FUS may produce synaptic dysfunction. *Tgfbr1* is one of the most significantly downregulated genes in both TDP-43-silenced neurons and FUS-silenced neurons (Table 2). Tgfbr1 encodes transforming growth factor (TGF)-β receptor I, which binds to TGF-β and transduces TGF-β signals from the cell surface to the cytoplasm. TGF-β signaling was disrupted in the motor neurons of mouse models of ALS and spinal and bulbar muscular atrophy (SBMA) [38,39]. This finding, in combination with our results, suggests that the TGF-β signaling pathway may be a strong candidate for targeted molecular therapy for motor neuron degeneration.

In addition, exon 14 of the *Camk2a* gene, which encodes the calcium/calmodulin-dependent protein kinase type II α chain, was skipped in both TDP-43-silenced primary neurons and FUS-silenced primary neurons. *Camk2a* is a critical player in calmodulin-dependent activity, long-term potentiation (LTP), and learning [40]. The expression of Camk2a has been reported to be decreased in Alzheimer's patients [41]. Clarifying the role of exon 14 of Camk2a in the function of this protein might link the calmodulin-dependent pathway to TDP-43- and FUS-associated FTLD. Despite the discovery of considerable evidence linking alternative splicing and various diseases, including neurodegeneration, it remains unclear how much alternative splicing is "noise" and how much of this splicing truly contributes to cell fate [42]. Further verification of whether these altered splicing events have pathogenic roles is required.

In this study, we determined that TDP-43-silenced neurons and FUS-silenced neurons exhibited greater overlap in shared gene expression alterations than in altered splicing events. In addition, a considerable number of GO terms from gene expression data were common to both types of neurons, whereas distinct GO terms were obtained from alternative splicing events in the two types of neurons. These results suggest that TDP-43 and FUS do not share many splicing targets but instead may associate with each other during mRNA maturation and/or transportation, resulting in altered gene expression. Another possibility is that TDP-43 and FUS may share common molecular pathways that lead to neuronal cell death after multiple transcriptome disturbances.

In summary, the comparative analysis of the transcriptome profiles in primary cortical neurons revealed common downstream RNA targets of TDP-43 and FUS. These targets may be linked to a common pathway in the neurodegenerative processes of ALS/FTLD.

Acknowledgments

Supplementary material

Supplementary material associated with this article can be found, in the online version, at doi:10.1016/j.fob.2013.11.001.

References

[1] Rothstein, J.D. (2009) Current hypotheses for the underlying biology of amyotrophic lateral sclerosis. Ann. Neurol. 65(Suppl. 1), S3–S9.

[2] Al-Chalabi, A., Jones, A., Troakes, C., King, A., Al-Sarraj, S. and van den Berg, L.H. (2012) The genetics and neuropathology of amyotrophic lateral sclerosis. Acta Neuropathol. 124, 339–352.

[3] Baloh, R.H. (2012) How do the RNA-binding proteins TDP-43 and FUS relate to amyotrophic lateral sclerosis and frontotemporal degeneration, and to each other? Curr. Opin. Neurol. 25, 701–707.

[4] Arai, T. (2006) TDP-43 is a component of ubiquitin-positive tau-negative inclusions in frontotemporal lobar degeneration and amyotrophic lateral sclerosis. Biochem. Biophys. Res. Commun 351, 602–611.

[5] Neumann, M. (2006) Ubiquitinated TDP-43 in frontotemporal lobar degeneration and amyotrophic lateral sclerosis. Science 314, 130–133.

[6] Gitcho, M.A. (2008) TDP-43 A315T mutation in familial motor neuron disease. Ann. Neurol. 63, 535–538.

[7] Sreedharan, J. (2008) TDP-43 mutations in familial and sporadic amyotrophic lateral sclerosis. Science 319, 1668–1672.

[8] Kabashi, E. (2008) TARDBP mutations in individuals with sporadic and familial amyotrophic lateral sclerosis. Nat. Genet. 40, 572–574.

[9] Yokoseki, A. (2008) TDP-43 mutation in familial amyotrophic lateral sclerosis. Ann. Neurol. 63, 538–542.

[10] Kwiatkowski, T.J. Jr. (2009) Mutations in the FUS/TLS gene on chromosome 16 cause familial amyotrophic lateral sclerosis. Science 323, 1205–1208.

[11] Vance, C. (2009) Mutations in FUS, an RNA processing protein, cause familial amyotrophic lateral sclerosis type 6. Science 323, 1208–1211.

[12] Buratti, E. and Baralle, F.E. (2012) TDP-43: gumming up neurons through protein–protein and protein–RNA interactions. Trends Biochem. Sci. 37, 237–247.

[13] Lagier-Tourenne, C. and Cleveland, D.W. (2009) Rethinking ALS: the FUS about TDP-43. Cell 136, 1001–1004.

[14] Strong, M.J. and Volkening, K. (2011) TDP-43 and FUS/TLS: sending a complex message about messenger RNA in amyotrophic lateral sclerosis? FEBS J. 278, 3569–3577.

[15] Davidson, Y., Kelley, T., Mackenzie, I.R., Pickering-Brown, S., Du Plessis, D., Neary, D. et al. (2007) Ubiquitinated pathological lesions in frontotemporal lobar degeneration contain the TAR DNA-binding protein, TDP-43. Acta Neuropathol. 113, 521–533.

[16] Neumann, M., Rademakers, R., Roeber, S., Baker, M., Kretzschmar, H.A. and Mackenzie, I.R. (2009) A new subtype of frontotemporal lobar degeneration with FUS pathology. Brain 132, 2922–2931.

[17] Wegorzewska, I., Bell, S., Cairns, N.J., Miller, T.M. and Baloh, R.H. (2009) TDP-43 mutant transgenic mice develop features of ALS and frontotemporal lobar degeneration. Proc. Natl. Acad. Sci. USA 106, 18809–18814.

[18] Igaz, L.M. (2011) Dysregulation of the ALS-associated gene TDP-43 leads to neuronal death and degeneration in mice. J. Clin. Invest. 121, 726–738.

[19] Iguchi, Y. (2013) Loss of TDP-43 causes age-dependent progressive motor neuron degeneration. Brain 136, 1371–1382.

[20] Kabashi, E., Bercier, V., Lissouba, A., Liao, M., Brustein, E., Rouleau, G.A. et al. (2011) FUS and TARDBP but not SOD1 interact in genetic models of amyotrophic lateral sclerosis. PLoS Genet. 7, e1002214.

[21] Wang, J.W., Brent, J.R., Tomlinson, A., Shneider, N.A. and McCabe, B.D. (2011) The ALS-associated proteins FUS and TDP-43 function together to affect Drosophila locomotion and life span. J. Clin. Invest. 121, 4118–4126.

[22] Wu, L.S., Cheng, W.C. and Shen, C.K. (2012) Targeted depletion of TDP-43 expression in the spinal cord motor neurons leads to the development of amyotrophic lateral sclerosis-like phenotypes in mice. J. Biol. Chem. 287, 27335–27344.

[23] Vanden Broeck, L. (2013) TDP-43 loss-of-function causes neuronal loss due to defective steroid receptor-mediated gene program switching in Drosophila. Cell Rep. 3, 160–172.

[24] Fujioka, Y. (2013) FUS-regulated region- and cell-type-specific transcriptome is associated with cell selectivity in ALS/FTLD. Sci. Rep. 3, 2388.

[25] Campeau, E. (2009) A versatile viral system for expression and depletion of proteins in mammalian cells. PLoS One 4, e6529.

[26] Ishigaki, S. (2012) Position-dependent FUS-RNA interactions regulate alternative splicing events and transcriptions. Sci. Rep. 2, 529.

[27] Huang da, W., Sherman, B.T. and Lempicki, R.A. (2009) Systematic and integrative analysis of large gene lists using DAVID bioinformatics resources. Nat. Protoc. 4, 44–57.

[28] Dennis, G. Jr., Sherman, B.T., Hosack, D.A., Yang, J., Gao, W., Lane, H.C. et al. (2003) DAVID: Database for Annotation, Visualization, and Integrated Discovery. Genome Biol. 4, P3.

[29] Van Langenhove, T., van der Zee, J. and Van Broeckhoven, C. (2012) The molecular basis of the frontotemporal lobar degeneration-amyotrophic lateral sclerosis spectrum. Ann. Med. 44, 817–828.

[30] Polymenidou, M., Lagier-Tourenne, C., Hutt, K.R., Bennett, C.F., Cleveland, D.W. and Yeo, G.W. (2012) Misregulated RNA processing in amyotrophic lateral sclerosis. Brain Res. 1462, 3–15.

[31] Polymenidou, M. (2011) Long pre-mRNA depletion and RNA missplicing contribute to neuronal vulnerability from loss of TDP-43. Nat. Neurosci. 14, 459–468.

[32] Sephton, C.F. (2011) Identification of neuronal RNA targets of TDP-43-containing ribonucleoprotein complexes. J. Biol. Chem. 286, 1204–1215.

[33] Rogelj, B. (2012) Widespread binding of FUS along nascent RNA regulates alternative splicing in the brain. Sci. Rep. 2, 603.

[34] Colombrita, C., Onesto, E., Megiorni, F., Pizzuti, A., Baralle, F.E., Buratti, E. et al. (2012) TDP-43 and FUS RNA-binding proteins bind distinct sets of cytoplasmic messenger RNAs and differently regulate their post-transcriptional fate in motoneuron-like cells. J. Biol. Chem. 287, 15635–15647.

[35] Lagier-Tourenne, C. (2012) Divergent roles of ALS-linked proteins FUS/TLS and TDP-43 intersect in processing long pre-mRNAs. Nat. Neurosci. 15, 1488–1497.

[36] Sorensen, J.B. (2005) SNARE complexes prepare for membrane fusion. Trends Neurosci. 28, 453–455.

[37] Mitchell, S.J. and Ryan, T.A. (2005) Munc18-dependent regulation of synaptic vesicle exocytosis by syntaxin-1A in hippocampal neurons. Neuropharmacology 48, 372–380.

[38] Nakamura, M., Ito, H., Wate, R., Nakano, S., Hirano, A. and Kusaka, H. (2008) Phosphorylated Smad2/3 immunoreactivity in sporadic and familial amyotrophic lateral sclerosis and its mouse model. Acta Neuropathol. 115, 327–334.

[39] Katsuno, M. (2010) Disrupted transforming growth factor-beta signaling in spinal and bulbar muscular atrophy. J. Neurosci. 30, 5702–5712.

[40] Giese, K.P., Fedorov, N.B., Filipkowski, R.K. and Silva, A.J. (1998) Autophosphorylation at Thr286 of the alpha calcium–calmodulin kinase II in LTP and learning. Science 279, 870–873.

[41] Wang, Y.J., Chen, G.H., Hu, X.Y., Lu, Y.P., Zhou, J.N. and Liu, R.Y. (2005) The expression of calcium/calmodulin-dependent protein kinase II-alpha in the hippocampus of patients with Alzheimer's disease and its links with AD-related pathology. Brain Res. 1031, 101–108.

[42] Kornblihtt, A.R., Schor, I.E., Allo, M., Dujardin, G., Petrillo, E. and Munoz, M.J. (2013) Alternative splicing: a pivotal step between eukaryotic transcription and translation. Nat. Rev. Mol. Cell Biol. 14, 153–165.
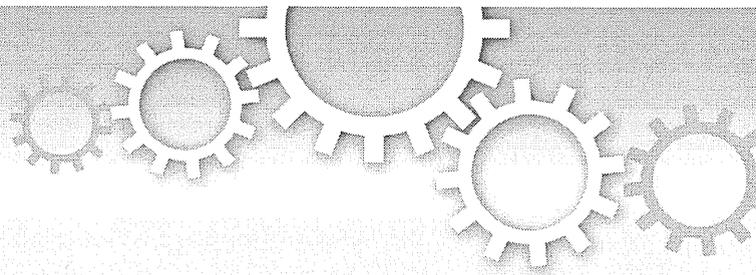
SCIENTIFIC REPORTS

FUS-regulated region- and cell-type-specific transcriptome is associated with cell selectivity in ALS/FTLD

Yusuke Fujioka[1], Shinsuke Ishigaki[1], Akio Masuda[2], Yohei Iguchi[1], Tsuyoshi Udagawa[1], Hirohisa Watanabe[1], Masahisa Katsuno[1], Kinji Ohno[2] & Gen Sobue[1]

[1]Department of Neurology, [2]Division of Neurogenetics, Center for Neurological Diseases and Cancer, Nagoya University Graduate School of Medicine, Nagoya, Japan.

FUS is genetically and pathologically linked to amyotrophic lateral sclerosis (ALS) and frontotemporal lobar degeneration (FTLD). To clarify the RNA metabolism cascade regulated by FUS in ALS/FTLD, we compared the FUS-regulated transcriptome profiles in different lineages of primary cells from the central nervous system. The profiles of FUS-mediated gene expression and alternative splicing in motor neurons were similar to those of cortical neurons, but not to those in cerebellar neurons despite the similarity of innate transcriptome signature. The gene expression profiles in glial cells were similar to those in motor and cortical neurons. We identified certain neurological diseases-associated genes, including Mapt, Stx1a, and Scn8a, among the profiles of gene expression and alternative splicing events regulated by FUS. Thus, FUS-regulated transcriptome profiles in each cell-type may determine cellular fate in association with FUS-mediated ALS/FTLD, and identified RNA targets for FUS could be therapeutic targets for ALS/FTLD.

A myotrophic lateral sclerosis (ALS) is a neurodegenerative disorder characterized by selective motor neuron death in adulthood. The etiology of ALS remains obscure, although many pathomechanisms have been suggested including RNA metabolism and non-cell autonomous toxicity[1,2]. While most ALS cases are sporadic, approximately 10–20% of ALS patients have a family history. In this regard, several genes have been identified as the cause or risk-factors for ALS, such as FUS and TAR DNA-binding protein (TDP-43), that are RNA binding proteins known to regulate RNA splicing and transcription[3,4]. Interestingly, accumulation of FUS and TDP-43 is observed in the cytoplasmic inclusions in sporadic ALS and frontotemporal lobar degeneration (FTLD), which is the second most common cause of presenile dementia[5,6]. Together with the evidence of FUS and TDP-43, which accumulate in cytoplasmic inclusions, the above studies strongly suggest that FTLD, ALS with dementia, and classical ALS are all parts of a clinicopathological spectrum of diseases characterized by disruption of RNA metabolism, which causes neurodegeneration in a subset of neurons in the central nervous system (CNS)[7].

How does loss-of-function and/or gain-of-toxicity cause neuronal cell death in diseases? Several lines of evidence indicate the involvement of loss-of-function in neurodegeneration observed in ALS/FTLD associated with FUS. Pathological studies have demonstrated FUS redistribution into the cytoplasm from the nucleus in sporadic and familial ALS as well as FTLD[8–10]. Other studies also showed the distribution of mutant FUS proteins associated with familial ALS in the cytoplasm from the nucleus, in contract to nuclear localization of endogenous and wild-type FUS[11–14]. Furthermore, the loss of FUS directly leads to neuronal cell death in drosophila[15] and zebrafish[16].

The cell selectivity in ALS/FTLD has remained a long-standing mystery. As mentioned above, the pathology of FUS-associated ALS/FTLD involves major selective neuronal vulnerability in both motor neurons and cortical neurons. Glial cells such as astrocytes and microglial cells are also likely to be involved in ALS/FTLD with regard to non-cell-autonomous toxicity[17–19]. On the other hand, cerebellar neurons are typically spared in ALS/FTLD. The expression pattern of FUS cannot explain the cell and region specific-selectivity in ALS/FTLD, since they are expressed ubiquitously throughout the CNS[8]. Based on this background, it is important to define Fus-targeting

RNA profiles in different cell lineages from the CNS for more precise interpretation of selective neuronal death in FUS-associated ALS/FTLD.

We reported recently that FUS regulates a subset of exon splicing events and gene expression in mouse primary cortical neurons in a position-dependent manner[20]. We also showed scattered binding of FUS to and around alternatively spliced exons, including those associated with neurodegeneration, such as *Mapt*, *Camk2a*, and *Fmr1*[20]. In the present study, we extend our research to the global roles of FUS on RNA metabolism in different cell lineages from the different CNS regions, including primary motor neurons, cortical neurons, glial cells, and cerebellar neurons, and describe a new pathomechanism of FUS-related ALS/FTLD.

Results

Lentivirus-mediated silencing of *FUS* in different cell lineages from the CNS.
We have described recently the establishment of Fus-silenced primary cortical neurons[20]. In order to compare RNA profiles of FUS in different cell types of the CNS, we prepared Fus-silenced primary motor neurons, primary cerebellar neurons, and primary glial cells by introducing lentivirus-expressing shRNA against Fus (shFUS) or scrambled control (Fig. 1A). The purity of each primary cell culture was confirmed by immunostaining for cell specific markers. We successfully established primary cultures of motor and cortical neurons with more than 95% purity. For primary glial cell cultures, we obtained astroctyes with purity of more than 95%, as confirmed by staining for GFAP. Both Purkinje cells and granule cells were the main cell populations among primary cerebellar neurons (Fig. 1B).

To exclude possible off-targeting effects, we used two different shRNAs, shFUS1 and shFUS2 in experiments performed in triplicate, as described in our recent study[20]. Correlation analysis between shFUS1 and shFUS2 showed a coefficient of determination (R^2) of 0.93 in primary cortical neurons, indicating that these two shRNA have minimal off-targeting effects[20]. The expression levels of *Fus* mRNA were efficiently suppressed in all four types of cells by both shFUS1 and shFUS2 by real-time quantitative PCR (Supplementary Fig. S1A). The FUS protein levels were decreased in all four types of cells by both shFUS1 and shFUS2 by immunoblot (Supplementary Fig. S1B). Immunohistochemistry also showed markedly decreased FUS protein levels in all four primary cells infected with shFUS1 and shFUS2 compared to shRNA against control scrambled oligonucleotides (shCont) (Supplementary Fig. S1C).

Innate gene expression profiles in neurons and glial cells.
The innate gene expression profiles of each cell-type infected with shCont were analyzed using the Affymetrix Mouse Exon 1.0 ST Array and compared by principal component analysis. The correlation coefficients were calculated (Supplementary Table S1) and summarized in the correlation plot and 2D-PCA scores (Fig. 1C). We found that the expression profiles of cerebellar neurons are very close to those of cortical neurons. The expression profiles of motor neurons are also similar to those of cortical neurons but with a lesser extent. On the other hand, the expression profiles of glial cells were divergent from those of the other three neuronal cells.

FUS regulates gene expressions in motor neurons, cortical neurons, and glial cells, but to a lesser extent in cerebellar cells.
In the next step, we analyzed the gene expression and alternative splicing events in Fus-silenced and control primary cells using the Affymetrix Mouse Exon 1.0 ST Array. To identify the common effects of Fus-silencing in different cell lineages from the CNS, we compiled a list of differentially expressed genes and differentially spliced exons in primary motor neurons, cortical neurons, glial cells, and cerebellar neurons, in which shFUS was introduced (GEO accession numbers: GSE36153 for cortical neurons, GSE42421 for motor neurons, glial cells, and

cerebellar neurons). We first prepared a list of FUS-regulated genes which were differentially expressed by shFUS for each cell lineage by filtering the gene-level signal intensities with t-test p values of ≤ 0.1. Then, we identified differentially expressed genes shared among the four primary types of cells.

The results of plot analysis of gene expression in primary cells of the CNS after Fus-depletion are shown in Fig. 2A. The numbers of differentially expressed genes with more than 1.3-fold change were higher in primary cortical neurons, motor neuron, and glial cells than in cerebellar neurons. Indeed, there were more than 2000 differentially expressed genes in these three cell types but only 494 genes in primary cerebellar neurons (Supplementary Table S2).

FUS-mediated gene expression profiles are similar between cortical and motor neurons and are less similar when these neuronal cells are compared to cerebellar neurons.
We investigated the similarity in differential gene expression profiles regulated by FUS among primary motor, cortical, and cerebellar neurons. Venn diagrams indicated overlap in genes or exons whose expression was regulated in the same direction by FUS (t-test, $p < 0.1$). Both motor and cortical neurons which are destined to die in ALS/FTLD, shared appreciable proportions of gene expression profiles (775/2321, 33.4% of genes in motor neurons; 775/2470, 31.4% of genes in cortical neurons). Cerebellar neurons, which are considered to be spared in ALS/FTLD, contained fewer numbers of FUS-regulated genes (t-test, $p < 0.1$) than motor and cortical neurons, and showed small overlapping rate with other neurons (58/494, 11.7% of genes with motor neurons; and 50/494, 10.1% of genes with cortical neurons) (Fig. 2B). The fold-changes in overlapped genes filtered by the t-test ($p < 0.1$) were plotted for primary motor, cortical, and cerebellar neurons. Comparison of gene expression profiles showed significantly high correlations between motor and cortical neurons ($R^2 > 0.80$, Fig. 2C: $p \leq 0.1$, by t-test, Supplementary Fig. S2A: $p \leq 0.075$ and 0.05, by t-test).

FUS-mediated alternative splicing profiles are similar in cortical and motor neurons but largely divergent compared with cerebellar neurons.
We next investigated the similarity in differential alternative splicing profiles regulated by FUS among primary motor, cortical, and cerebellar neurons. We filtered the exon-level signal intensities with t-test p values ≤ 0.1, and prepared a list of FUS-regulated exons for each cell lineage and identified shared FUS-regulated exons. In alternative splicing profiles, about 10% (965/10727, 9.0% of genes in motor neurons; and 965/8183, 11.8% of genes in cortical neurons) of genes showed overlap between motor and cortical neurons at the exon levels, whereas cerebellar neurons showed only overlap in about 4% (434/9907, 4.4% of genes with motor neurons; and 325/9907, 3.3% of genes with cortical neurons) of genes at the exon levels compared with the other two neurons (Fig. 2B). The overlapped exons filtered by the t-test were also plotted for primary motor, cortical, and cerebellar neurons. Comparisons of exon splicing profiles showed a significant correlation only between motor and cortical neurons ($R^2 > 0.7$), but not between motor and cerebellar neurons, or cortical and cerebellar neurons ($R^2 < 0.1$, each) (Fig. 2C: $p \leq 0.1$, by t-test, Supplementary Fig. S2B: $p \leq 0.075$ and 0.05, by t-test).

Glial cells are similar to motor and cortical neurons in FUS-regulated gene expression profiles but not in alternative exon profiles.
Glial cells, which are thought to be the modifier in ALS/FTLD, were also investigated with regard to similarity to motor and cortical neurons in differential gene expression and alternative splicing profiles regulated by FUS. Venn diagrams showed that the gene expression profiles of glial cells shared certain similarities with motor and cortical neurons (422/2074, 20.3% of genes with motor neurons; 453/2074, 21.8% of genes with cortical neurons, Fig. 2D). Comparison of gene expression profiles in the plot analysis showed positive correlations between glial cells and both motor and cortical
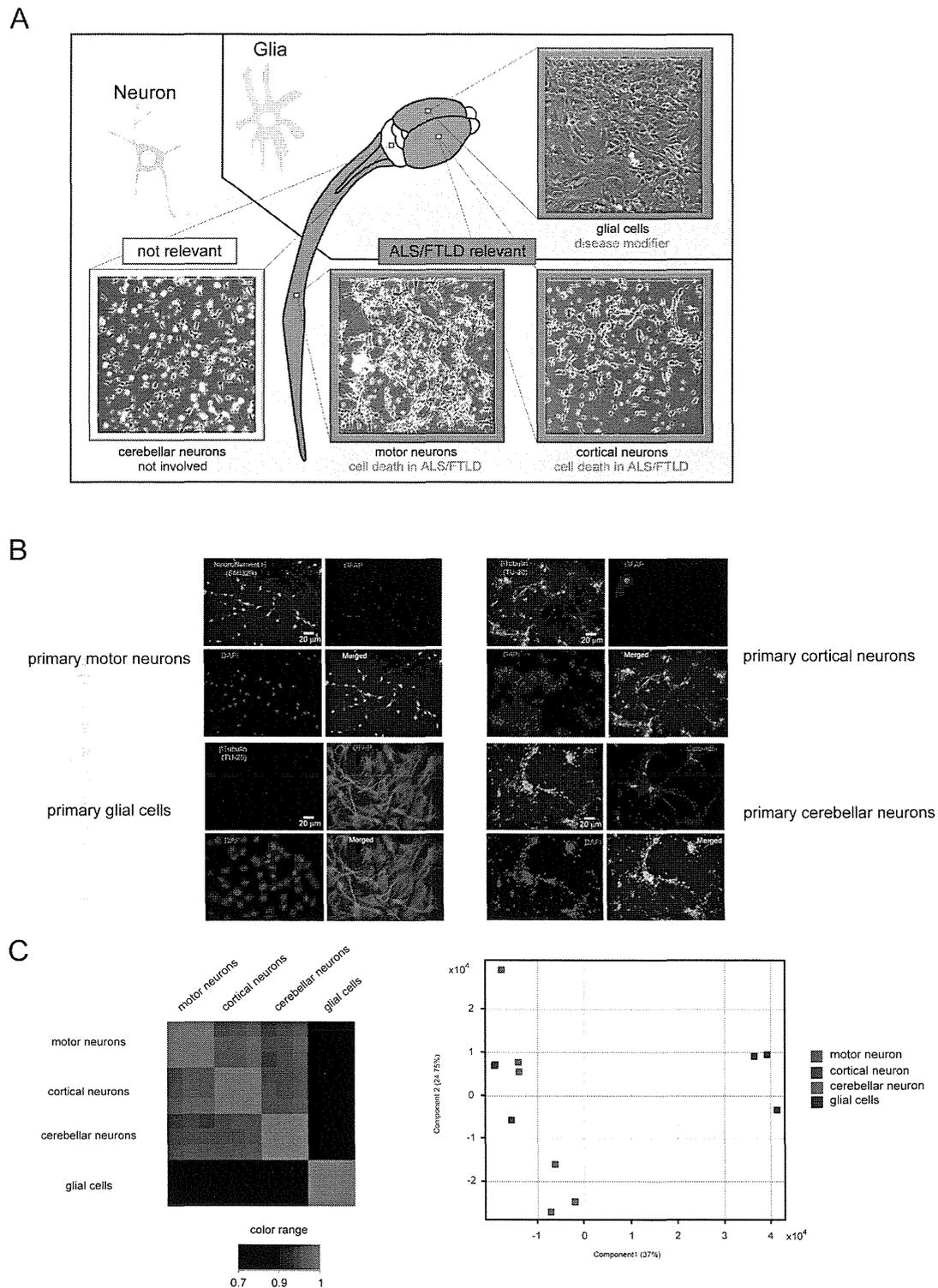
Figure 1 | Experimental schema and characterization of four primary cells from the central nervous system. (A) Primary motor neurons were harvested from the spinal cords of C57BL/6 mouse embryos at embryonic E13. Primary cortical neurons and primary glial cells were obtained from the cerebrum of C57BL/6 mouse at E15. Primary cerebellar neurons were obtained from the cerebellum of C57BL/6 mouse at E15. Motor and cortical neurons, but not cerebellar neurons, are affected in ALS/FTLD. Glial cells are disease-modifiers in ALS/FTLD. Primary cells were infected with lentivirus expressing two different shRNAs against FUS (shFUS1 and shFUS2) and control shRNA (shCont). Total RNA was isolated and analyzed by the Affymetrix Mouse Exon Array. Each experiment was performed in triplicate. (B) The purity of primary motor neurons, primary cortical neurons, primary glial cells, and primary cerebellar neurons was confirmed by immunostaining using specific antibodies: anti-neurofilament-H antibody (SMI32R) for primary motor neurons; anti-β tubulin antibody (TU20) for primary cortical neurons; anti-GFAP antibody for glial cells; anti-Zic1 antibody for granule cells in primary cerebellar neurons; and anti-calbindin antibody for Purkinje cells in primary cerebellar neurons. (C) The innate gene expression profiles of each cell type introduced with shCont were compared by principal component analysis (n = 3 for each cell-type). The correlation coefficients were calculated (Supplementary Material, Table S1) and summarized in the correlation plot (left). The 2D PCA scores and the loadings plots of the innate gene expression profiles of each cell-type introduced with shCont indicated that significant separation between the profiles of the three primary neurons and that of glial cells (right).
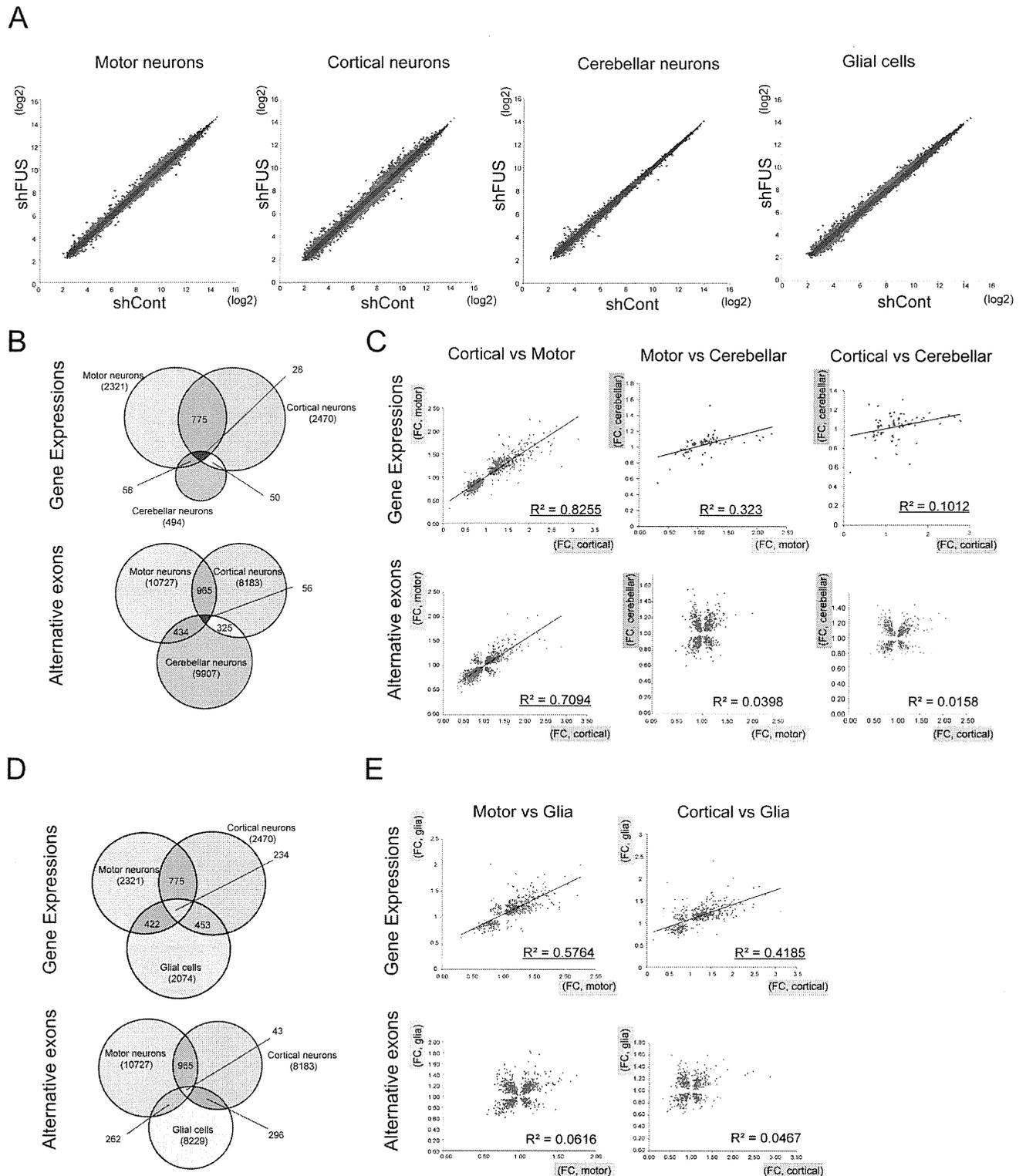
- 105 -

Figure 2 | Comparison of gene expression and exon splicing profiles among different cell lineages from the central nervous system after *Fus* knockdown. (A) Scatter plot analysis of gene expression using shCont and shFUS in different primary cells from the central nervous system. Genes whose expression levels changed by more than 1.3-fold after Fus-silencing with shFUS1 are indicated in red. (B) The profiles of gene expression and alternative splicing events were compared among the three different primary neurons. Venn diagrams indicate overlap in genes (*top*) and exons (*bottom*) whose expression levels are uniquely or concordantly regulated by FUS among motor, cortical, and cerebellar neurons ($p < 0.1$, by t-test). (C) The fold-changes in overlapped genes filtered by the t-test ($p < 0.1$) were plotted for primary motor, cortical, and cerebellar neurons. Scatter plots of fold-changes in gene expression levels (*top*) and alternative splicing events (*bottom*) after *Fus* knockdown. The R^2 value was calculated for genes and exons with t-test p values < 0.1. (D) As in Fig. 2B, the profiles of gene expression and alternative splicing events in glial cells were compared with those of motor and cortical neurons. Venn diagrams indicate overlap in genes (*top*) and exons (*bottom*) whose expression levels are uniquely or concordantly regulated by FUS among motor, cortical, and glial cells ($p < 0.1$, by t-test). (E) Scatter plots of fold-changes in gene expression levels (*top*) and alternative splicing events (*bottom*) after *Fus* knockdown. The R^2 value was calculated for genes and exons with t-test p values < 0.1.

neurons ($R^2 = 0.58$ and 0.42, respectively). On the other hand, comparisons of exon splicing profiles did not show a significant correlation between motor neurons and glial cells, and cortical neurons and glial cells ($R^2 < 0.1$, each, Fig. 2E). Thus, FUS regulates the expression levels and alternative splicing of the largest number of shared genes between cortical and motor neurons. Similarly, though less concordantly, FUS regulates the expression levels of the same genes among the cortical/motor, cerebellar, and glial cells, but not alternative splicing of these cells.

Characterization of genes with altered gene expression and spliced alternative exon regulated by FUS in different cell lineages of the

CNS. We also analyzed Gene Ontology (GO) terms of genes shown in the Venn diagrams using DAVID 6.7[21,22]. The GO terms of genes regulated by FUS in primary motor neurons were mainly those involved in signaling cascades and metabolic processes that were similar to those in primary cortical neurons (Table 1). The GO terms of those in glial cells are mainly involved in the regulation of the immune system. The GO terms of those in cerebellar neurons were not available since the number of differentially expressed genes was too small. The GO terms of genes involved in FUS-related regulation of alternative splicing events in both motor and cortical neurons were mainly involved in various neuronal functions such as synapse, nerve impulse, and neuronal projection. In contrast, none of

Table 1 | Gene Ontology terms for FUS-associated genes in each primary cell type

	GO ID	Term	P value
Gene expression			
Motor neurons			
	GO:0008104	protein localization	0.002392
	GO:0006796	phosphate metabolic process	0.002963
	GO:0006793	phosphorus metabolic process	0.002963
	GO:0015031	protein transport	0.006112
	GO:0045184	establishment of protein localization	0.006463
	GO:0016310	phosphorylation	0.012273
	GO:0006468	protein amino acid phosphorylation	0.014793
Cortical neurons			
	GO:0019637	organophosphate metabolic process	3.68E-04
	GO:0006644	phospholipid metabolic process	4.89E-04
	GO:0016055	Wnt receptor signaling pathway	5.21E-04
	GO:0009100	glycoprotein metabolic process	5.30E-04
	GO:0007264	small GTPase mediated signal transduction	5.91E-04
	GO:0006650	glycerophospholipid metabolic process	8.42E-04
	GO:0007242	intracellular signaling cascade	0.001227
Glial cells			
	GO:0009615	response to virus	1.68E-08
	GO:0006955	immune response	1.18E-07
	GO:0048525	negative regulation of viral reproduction	0.012033
	GO:0006952	defense response	0.01839
	GO:0045087	innate immune response	0.026843
	GO:0008653	lipopolysaccharide metabolic process	0.035673
	GO:0050792	regulation of viral reproduction	0.047282
Alternative splicing			
Motor neurons			
	GO:0006836	neurotransmitter transport	0.003894
	GO:0007268	synaptic transmission	0.018152
	GO:0032940	secretion by cell	0.019717
	GO:0046903	secretion	0.027201
	GO:0019226	transmission of nerve impulse	0.028352
	GO:0007269	neurotransmitter secretion	0.041581
	GO:0007267	cell-cell signaling	0.044736
Cortical neurons			
	GO:0045202	synapse	6.85E-07
	GO:0042995	cell projection	2.54E-06
	GO:0043005	neuron projection	2.29E-05
	GO:0005856	cytoskeleton	1.73E-04
	GO:0005886	plasma membrane	1.88E-04
	GO:0043232	intracellular non-membrane-bounded organelle	2.07E-04
	GO:0043228	non-membrane-bounded organelle	2.07E-04
Glial cells			
	GO:0030097	hemopoiesis	0.006476
	GO:0048534	hemopoietic or lymphoid organ development	0.008832
	GO:0002520	immune system development	0.010084
	GO:0030098	lymphocyte differentiation	0.013204
	GO:0002521	leukocyte differentiation	0.019998
	GO:0007517	muscle organ development	0.029812
	GO:0046649	lymphocyte activation	0.034644
Cerebellar neurons			
	GO:0051301	cell division	0.006634
	GO:0046632	alpha-beta T cell differentiation	0.026253
	GO:0046631	alpha-beta T cell activation	0.031696

the neuronal function terms emerged in the list of alternative splicing events in cerebellar neurons. Alternative splicing events in glial cells were mostly categorized into immunohematological functions (Table 1).

Supplementary Table S3 lists the top 10 genes that were differentially expressed in Fus-silenced motor neurons, together with the fold-change values in cortical neurons, glial cells, and cerebellar neurons. Similar to the global profile comparison shown in Fig. 2, the expression patterns of genes in the three different primary cells were similar except for cerebellar neurons, whose profile was less altered by Fus-depletion than other cell types.

After filtering exons with genes that were differentially expressed by both shFUS1 and shFUS2 with t-test p value of ≤ 0.1 and with fold-changes ≥ 1.3-fold in each primary cell, we categorized alternative splicing exons into category "A" to "E". In total, 44 exons were validated by RT-PCR and shown in Table 2, Fig. 3A–C, and Supplementary Fig. S3A–E. Alternative splicing exons A were specific to primary cortical neurons and primary motor neurons; B,

specific to primary motor neurons; C, specific to primary cortical neurons; D, specific to primary glial cells, E, were common among primary motor neurons, cortical neurons, glial cells and/or cerebellar neurons.

We identified 18 alternative splicing events that were motor- and cortical neuron-specific, including *Mapt*, *Dlgap4*, and *Snap25* (Fig. 3A). All the validated splicing events that were motor- and cortical neuron-specific are shown in Supplementary Fig. S3A. We observed motor-neuron-specific alternative splicing events in *Synj1*, *Scn8a*, and *Rims1* (Fig. 3B). We also identified several alternative spliced events that were differentially expressed in Fus-silenced cortical neurons. Fig. 3C shows representative cortical-neuron-specific alternative splicing events in *Kcnip*, *Stxbp1*, and *Fmr1*. All the validated events are shown in Supplementary Fig. S3C. Furthermore, Glial-cell-specific alternative splicing events were seen in *Sgce*, *Wdr35*, and *Fip1l1* (Supplementary Fig. S3C). Exons in *Fxr1* and *Tsc22d2* were alternatively spliced in all primary cell types. *Map4* exon14 inclusion was also observed in primary cortical neurons,

Table 2 | List of validated FUS-regulated cell-type specific alternative splicing events

gene symbol	alternative splicing	motor neurons	cortical neurons	glial cells	cerebellar neurons	group
Mapt	Ex10 inclusion	✓	✓	-	-	A
Dlgap1	Ex10 inclusion	✓	✓	-	-	A
Snap25	Alternative exon (Ex5)	✓	✓	-	-	A
Anks1b	Ex7 inclusion	✓	✓	-	-	A
Brcc3	3′UTR elongation	✓	✓	-	-	A
Tia1	Ex5 inclusion	✓	✓	-	-	A
Caskin1	Ex15-16 skipping	✓	✓	-	-	A
Clec16a	Ex10 shortening	✓	✓	-	-	A
Elmo2	Ex10 skipping	✓	✓	-	-	A
Erc2	Ex12 skipping	✓	✓	-	-	A
Fkbp15	Ex19 elongation	✓	✓	-	-	A
Grm5	Ex8 inclusion	✓	✓	-	-	A
Lrrc7	Ex23 skipping	✓	✓	-	-	A
Pdzd4	Ex2-3 skipping	✓	✓	-	-	A
Smarca1	Ex3 alternative exon	✓	✓	-	-	A
Tcerg1l	Ex7 elongation	✓	✓	-	-	A
Xpr1	Ex13 elongation	✓	✓	-	-	A
Anks1	Ex24 skipping	✓	✓	-	-	A
Synj1	Ex27 inclusin	✓	-	-	-	B
Rims1	Alternative 3′-UTR	✓	-	-	-	B
Scn8a	Alternative exon (Ex4)	✓	-	-	-	B
Stxbp1	Ex19 skipping	-	✓	-	-	C
Kcnip1	Ex2 skipping	-	✓	-	-	C
Fmr1	Ex12 inclusion	-	✓	-	-	C
Abi1	Ex8 skipping	-	✓	-	-	C
CamK2a	Ex14 skipping	-	✓	-	-	C
Cttn	Ex11 skipping	-	✓	-	-	C
Grip1	Ex10 inclusion	-	✓	-	-	C
Nav2	Ex5 inclusion	-	✓	-	-	C
Neo1	Ex26 skipping	-	✓	-	-	C
Ndrg3	Ex16 skipping	-	✓	-	-	C
Rapgef4	Ex7 inclusion	-	✓	-	-	C
Sh3kbp1	Ex6-7 inclusion	-	✓	-	-	C
Slc1a2	Ex11 skipping	-	✓	-	-	C
Ttll5	Ex33 skipping	-	✓	-	-	C
Zhx1	Ex3 skipping	-	✓	-	-	C
Braf	Ex12 skipping	-	✓	-	-	C
Wdr35	Ex11 inclusion	-	-	✓	-	D
Sgce	Ex2 inclusion	-	-	✓	-	D
Fip1l1	Ex9 inclusion	-	-	✓	-	D
Fxr1	Ex15-16 inclusion	✓	✓	✓	✓	E
Tsc22d2	Ex2 inclusion	✓	✓	✓	✓	E
Map4	Ex14 inclusion	✓	✓	✓	-	E
Ntng1	Ex7 inclusion	✓	✓	-	✓	E

✓:changed significantly with Fus silencing.
A: specific to primary cortical neurons and primary motor neurons; B, specific to primary motor neurons; C, specific to primary cortical neurons; D, specific to primary glial cells, E, common among primary motor neurons, cortical neurons, glial cells and/or cerebellar neurons.
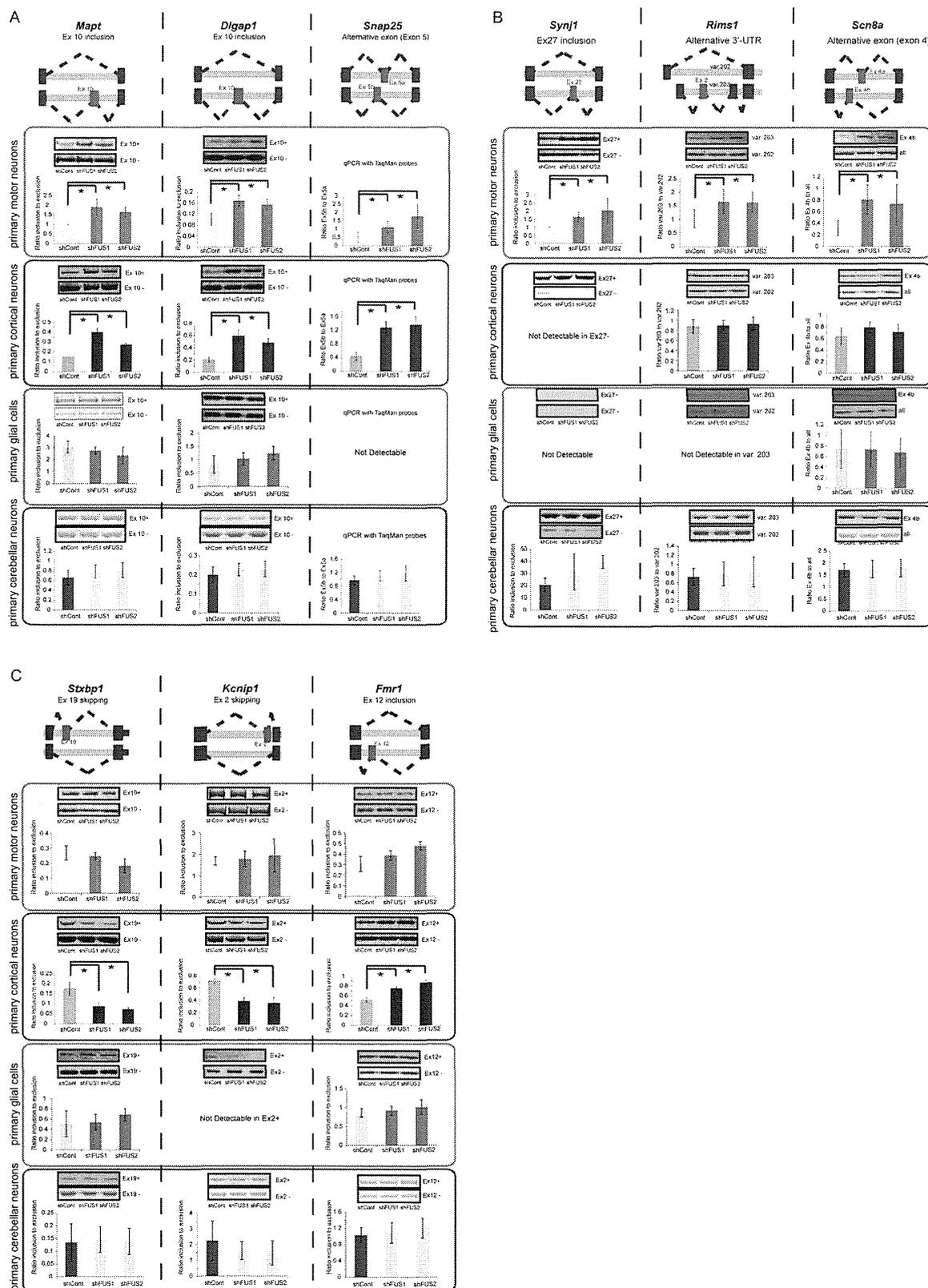
Figure 3 | Validation of representative altered splicing events in different cell lineages from the central nervous system after *Fus-silencing*. (A–C) Three representative alternative splicing events regulated by Fus are shown in each category: (A) both motor and cortical neuron-specific, (B) motor neuron-specific, and (C) cortical neuron-specific. All the validation of altered splicing events including category D and E, are shown in Supplementary Fig. S3. The top panels represent schematic splicing changes mediated by FUS. shCont and shFus resulted in splicing events shown in the top and bottom rows, respectively. The second panels show representative RT-PCR of the indicated exons in primary motor neurons. Similarly, the third, fourth, and fifth panels show representative RT-PCR of the indicated exons in primary cortical neurons, primary glial cells, and primary cerebellar neurons, respectively. The experiments were repeated four times using four independent sets of samples. The results of densitometric quantification of RT-PCR are shown in bar graphs (n = 4; mean ± SD). *p < 0.05, between shCont and shFUS (by Student's t-test).

motor neurons, and glial cells; but not in cerebellar neurons (Supplementary Fig. S3D).

Interestingly, we also identified many neurological disease-associated genes among the profiles of gene expression and alternative splicing events. We list such representative genes in Table 3.

The protein levels of representative genes with altered spliced events and gene expression were validated by immunoblot in all four primary cells in the CNS (Fig. 4). The expression of 4-repeat Tau (RD4) which corresponds to the exon10 (+) isoform of *Mapt* gene was increased by shFUS in primary cortical neurons but was undetectable in motor neurons. On the other hand, the expression of 3-repeat Tau (RD3) which corresponds to the exon10 (-) isoform was decreased in primary cortical and motor neurons. The 89kD form of Braf protein encoded by the exon12 (+) variant of *Braf* gene was decreased in Fus-silenced primary cortical neurons. The protein expression level of Syntaxin-1A was upregulated in Fus-silenced cortical and motor neurons as observed in its mRNA levels.

Direct binding of FUS to target mRNA was not tisseue-type specific in CNS. To investigate the direct binding of FUS to mRNA of the genes and exons with altered expression, RNA immunoprecipitation (RIP) using differenet tissues of CNS was performed. We prepared the spinal cord (E13), the cerebrum (E15), and the cerebellum (E15) from the mouse embryos, and FUS protein was immunoprecipitated from each tissue (Fig. 5A). FUS-associated mRNA levels were evaluated by RT-PCR using specific primers for *Mapt*, *Dlgap1*, and *Stxbp1*, of which alternative splicing events were regulated by FUS. Primers for *Gapdh* and intergenic region were used as negative controls. The RIP results showed that the interaction levels between FUS and mRNA of *Mapt*, *Dlgap1*, and *Stxbp1* among three different CNS tissues were comparable, whereas these three genes showed cell-type specific splicing patterns in Fig 3 (Fig. 5B). There was no apparent binding of FUS to *Gapdh* mRNA or intergenic region (Fig. 5B). We next analyzed position dependence of FUS-binding to splicing targets and their effects on alternative splicing through comprehensive analysis of the exon array using primary glial cells and HITS-CLIP of mouse brain (Fig. 5C–D). We analyzed the positions of CLIP-tags of 121 FUS-responsive exons (29 exon skipped and 92 exon included by shRNA) that were filtered by t-test p value ≤ 0.1 and fold-change of ≤0.67 or ≥1.5 for shFUS1. We combined these exons into a single composite pre-mRNA and prepared integrated RNA maps from our HITS-CLIP reads mapped to the corresponding genomic regions, as described in more detail previously[23–25]. The analysis showed that scattered FUS binding sites mainly around the alternatively spliced exons. Conspicuous binding of FUS was observed at ~500 nt upstream of the 3' end of the downstream intron in skipped exons (arrows in Fig. 5C). This finding was similar to the complexity map of primary cortical neurons that was reported previously by our group (Fig. 5D)[20].

Discussion

In the present study, we determined the gene expression profiles and alternative splicing events in four different primary cells of the CNS, with silenced *Fus* induced by lentivirus encoding shRNA against *Fus*. By comparing the gene expression profiles of the four primary cells, we found that the genes altered by Fus-silencing were fewer in cerebellar neurons than in the other three cell types, although the innate gene expression profiles of motor, cortical and cerebellar neurons were similar. These findings suggest that gene expression profile reflects cellular response affected by Fus-silencing in each cell type, given that ALS/FTLD-relevant cell types showed more alterations than non- ALS/FTLD-relevant cell type. On the other hand, the profiles of alternative splicing events were only similar in motor and cortical neurons. Alternative splicing events in these two types of neurons were far different from glial cells and cerebellar neurons, suggesting that alternative splicing events are uniquely fine-tuned in a cell-specific manner (Fig. 2). Alternative splicing contributed to brain development in mammals during the evolution process[26,27]. In the adult human, the brain expresses more alternatively spliced transcripts than any other tissues[28], and the majority of splicing events are regulated in a tissue-specific manner[29]. Our finding that FUS-regulated alternative splicing events were more region- and cell-type-specific than those of gene expression suggests that the profiles of alternative splicing events may reflect direct phenomenon caused by Fus-depletion whereas those of gene expression include both indirect phenomenon as well as direct suppressive effects on transcription by binding to promoter antisense transcripts[20]. Indeed, we observed more frequent FUS-tagged sites on genes with altered spliced alternative exons than genes with altered gene expression (Supplementary Fig. S4). In this context, the alternative splicing events regulated by FUS could explain the cell vulnerability in ALS/FTLD associated with FUS, whereas the gene expression regulated by FUS could represent the size of cellular impact in FUS-associated ALS/FTLD. The fact that cell death broadly occurs in the cerebral cortex but not in the cerebellum and that cell death occurs only in neurons but not in glial cells in ALS/FTLD also supports this notion[30,31]. Although we found cell-type-specific profiles of FUS-regulated alternative splicing events, the RIP experiments showed that direct interaction between FUS and target RNA was comparable in different CNS tissues. The complexity map showed similar patterns for FUS-binding positions around the alternatively spliced exons in cortical neurons and glial cells. These findings indicate that FUS binding to mRNA is not dependent on cell/tissue type. Instead, other molecules that associate with FUS in the spliceosome are likely to dictate cell/tissue type-specificity of FUS-mediated alternative splicing events. FUS protein-interaction analysis may provide more detail information about cell specific machinery of FUS on alternative RNA splicing.

Table 3 | List of FUS-regulated genes/exons in various neurological disease

Gene	Effect by Fus-silencing	Cell type	Neurological Disease	Neuronal Function
Mapt	Ex10 inclusion	motor/cortical	FTLD	microtuble stabilization
Fmr1	Ex12 inclusion	cortical	Fragile X	Translation repressor
Fxr1	Ex15−16 inclusion	all	Fragile X	RNA-binding protein
Stx1a	upregulation	motor/cortical	Williams-Beuren syndrome	Part of the SNARE core complex
Snap25	Ex5 alternative exon	motor/cortical		Part of the SNARE core complex
Stxbp1	Ex19 skipping	cortical	EIEE4	binding to syntaxins
Camk2a	Ex14 skipping	cortical	Alzheimer's disease	LTP
Scn8a	Ex4 alternative exon	motor	EIEE13	sodium channel
Sgce	Ex2 inclusion	glial	Myoclonus dystonia	dystrophin-glycoprotein complex
Fktn	downregulation	all	Congenital muscular dystrophy	glycosyltransferase

EIEE4: epileptic encephalopathy early infantile type 4.
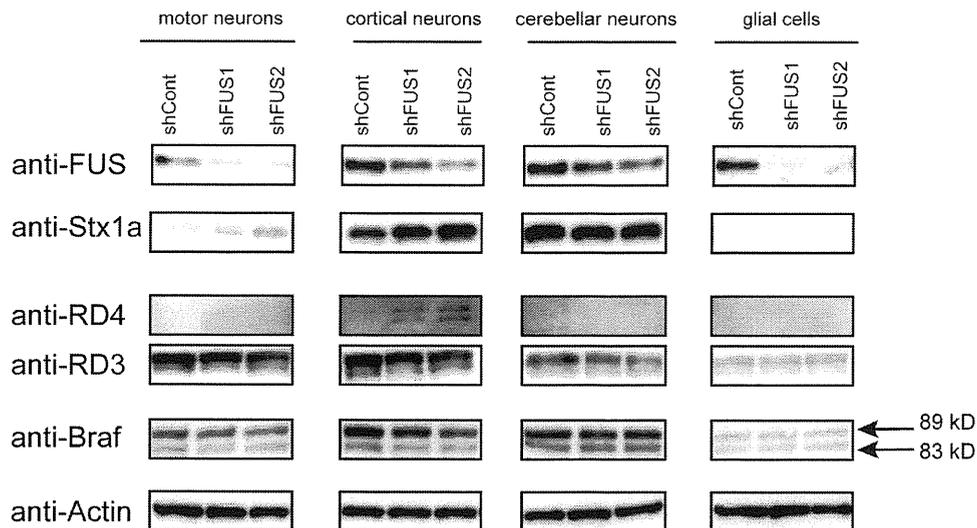EIEE13: epileptic encephalopathy early infantile type 13.

Figure 4 | Protein expressions of genes with altered splicing events and gene expression in different cell lineages from the central nervous system after *Fus*-silencing. Protein levels of representative genes with altered splicing events (Tau and Braf) and gene expression (Syntaxin-1A) were evaluated in different primary cells in the CNS with Fus-silencing. Expression levels of FUS, Syntaxin-1A (Stx1a), 3-repeat Tau (RD3), 4-repeat Tau (4RD), Braf, and actin were measured by immunoblot.

The results showed concordant regulation of many alternative splicing events by FUS in both motor and cortical neurons, which underscores the notion that FUS-mediated ALS and FTLD could be considered the same disease entity based on clinicopathological and genetic findings[7,32]. The cell-type specific transcriptome profiles we established were embryonic; however many of identified FUS-mediated splicing events were likely to be seen in adult tissues. Indeed, 34% (15/44) of alternative splicing events in Table2 were also seen in the list of another report[33] using adult mouse brain with Fus-silencing (data not shown). Among them, *Mapt* is the most notable gene whose splicing was affected by Fus-depletion (Fig. 3A and Table 2). The inclusion exon 10 yields 4-repeat Tau (RD4), whereas skipping of exon10 generates 3-repeat Tau (RD3). We reported previously the increase of exon 10 inclusion in *Mapt* in Fus-silenced primary cortical neurons, a finding also reported by several other groups[20,33-35]. In this study, we also found the increase of exon 10 inlusion in primary motor neurons, although the protein level of RD4 was only dectable in cortical neurons. In this regard, it is intriguing that previous studies reported the presence of high RD4/RD3 ratio in various neurodegenerative disorders, including FTLD[36,37]. However, little is known about the involvement of Tau pathology in motor neuron degeneration in ALS. Further studies are necessary to clarify the association between the FUS-Tau pathway and pathogenesis of ALS and FTLD.

As described above, the entire profiles of alternative splicing events in motor and cortical neurons were almost identical. Nonetheless, we identified only motor neuron- or cortical neuron-specific alternative splicing events with close observation of region- and cell-type specific profiles of alternative splicing. Those splicing events may potentially represent differences in cell fate in each clinical subtype of ALS/FTLD. We identified some channel-associated genes, such as *Synj1*, *Scn8a*, and *Rims1* as motor neuron-specific alternative splicing targets regulated by FUS (Fig. 3B and Table 2), indicating that synaptic dysfunction provoked by Fus-silencing seems to be one of causes of motor neuron degeneration.

On the other hand, cortical neuron-specific alternative exons might affect cerebral neurons, leading to cortex pathology in FTLD. *Stxbp1* is the causative gene for epileptic encephalopathy early infantile type 4 (EIEE4)[38] and participates in the regulation of synaptic vesicle docking and fusion by associating with the SNARE complex, which is essential for fusion of opposing cellular

membranes necessary for neurotransmission[39]. It is noteworthy that two other SNARE complex components; Syntaxin-1A and Snap25, were also identified as FUS-regulated gene and alternative exon, respectively (Fig. 3C and Table 2). Fmr1 is essential for normal cognitive development and its mutation can lead to fragile X syndrome characterized by mental retardation, autism, Parkinson's disease, and other cognitive deficits[40]. The other fragile X syndrome-related gene, *Fxr1*, is also included among the list of alternative exons in which *Fxr1* exon 16 is skipped by Fus-silencing in all cell types (Supplementary Fig. S3D and Table 3).

Involvement of glial cells, such as astrocytes and microglia, likely modifies and exaggerates the ALS/FTLD disease process. Although it is not clear whether non-cell autonomous mechanism is also relevant to FUS-associated ALS/FTLD, we showed here that primary glial cells showed more altered differential genes by Fus-silencing than cerebellar neurons (Fig. 2A), suggesting that knock-down of FUS gene could have certain impact on cellular homeostasis of glial cells, in addition to motor and cortical neurons.

Our global analysis also identified several genes relevant to various neurological diseases (Table 3). The alteration of gene expression and/or alternative splicing of these genes may have a large impact on neuronal function. It is unlikely that only one of these genes or exons is solely responsible for neurodegeneration in ALS/FTLD. FUS silencing would have a partial effect instead of total loss of function by altering isoforms or down/up regulation of these genes; therefore, it is possible that accumulation of altered genes affected by FUS-depletion could cause neurodegeneration after reaching a critical threshold level even when the individual alternative splicing event and gene expression are not critical by themselves. Investigation of FUS-targeting molecules, especially those relevant to neurological diseases may provide mechanistic insights into selective neuronal degeneration in FUS-associated ALS/FTLD.

Methods

Primary cells from the central nervous system. Primary motor neurons were harvested from the spinal cords of C57BL/6 mouse embryos at embryonic (E) day 13. Primary cortical neurons and primary glial cells were obtained from the cerebri of C57BL/6 mice at E15. Primary cerebellar neurons were obtained from cerebelli of C57BL/6 mice at E15. The procedure for culture of each primary cell and lentivirus infection are described in the online supplementary information. All animal experiments were performed in accordance with the National Institutes of Health Guide for the Care and Use of Laboratory Animals and under the approval of the Nagoya University Animal Experiment Committee (Nagoya, Japan).
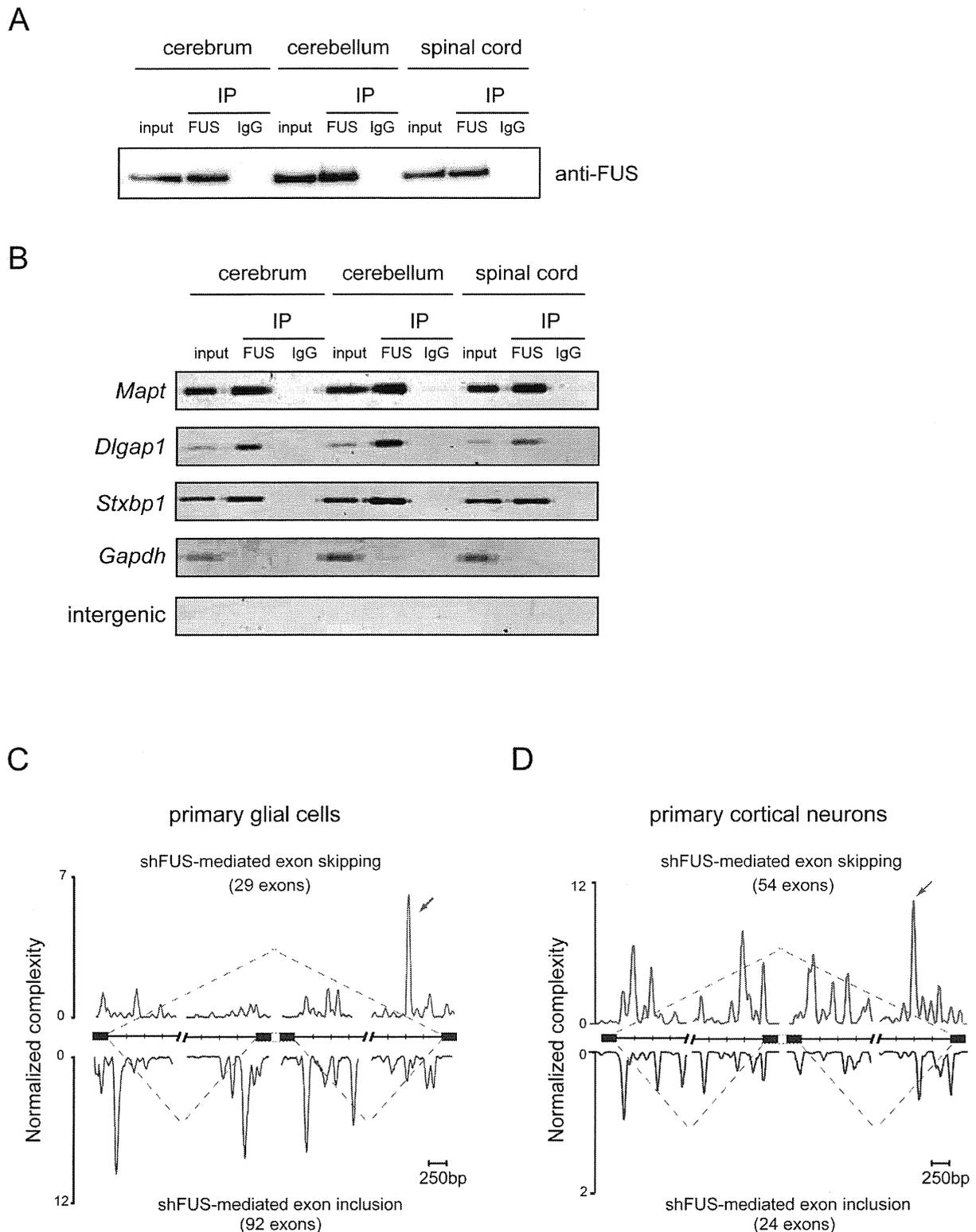
Figure 5 | The binding of FUS to mRNA is not tissue and cell type specific in the CNS. (A–B) RNA immunoprecipitation (RIP) was performed to detect the interaction between FUS and mRNA of genes with altered splicing events using mouse cerebrum, cerebellum, and spinal cord. (A) Anti-FUS immunoblot of 1% input, FUS-IP, and control IP (IgG) from mouse cerebrum, cerebellum, and spinal cord at E15 embryos was shown. (B) FUS-associated RNA was reverse transcribed and evaluated by semi-quantative PCR with specific primers for three representative FUS-target genes with altered alternative splicing events, Mapt, Dlgap1, and Stxbp1. Primers for Gapdh and intergenic region (intergenic) were used as controls. (C–D) We compared normalized complexity map of FUS-dependent splice sites of primary glial cells and cortical neurons. shFUS-mediated alternative splicing events in primary glial cells (C) and primary cortical neurons (D) are compiled. Blue arrows point to conspicuous peaks at ~500 nt upstream of the 3′ end of the downstream intron. The complexity map of primary cortical neuron (D) is identical to that shown in the Supporting Information/Fig. S3 in our previous report[20], which is shown for comparison with that of primary glial cells (C).

- 112 -

Lentivirus. We designed two different shRNAs against mouse *Fus* as well as a control shRNA. The targeted sequences were 5'-GCAACAAAGCTACGGACAA-3' for shRNA/FUS1 (shFUS1); 5'-GAGTGGAGGTTATGGTCAA-3'for shRNA/FUS2 (shFUS2); and 5'-AATTCTCCGAACGTGTCACGT-3' for shRNA/control (shCont). These were cloned into a lentiviral shRNA vector (pLenti-RNAi-X2 puro DEST, w16-1, a kind gift from Dr. Eric Campeau at Resverlogix Corp., Calgary, Alberta, Canada). Lentivirus was prepared using the protocol described by Campeau et al[41]. Briefly, lentiviral particles were produced in HEK293T cells by transfection using Lipofectamine 2000 (Invitrogen, Carlsbad, CA). The lentivirus-containing supernatant was collected at 48 hours after transfection, and stored at −80°C. Lentivirus titer was measured using NucleoSpin RNA Virus kit (Clontech, Mountain View, CA).

Microarray analysis. Total RNA was extracted from primary motor neurons, cortical neurons, cerebellar neurons, and glial cells by the RNeasy Mini kit (Qiagen, Hilden, Germany). We confirmed that the RNA integrity numbers (RIN) were all above 7.0. cDNA fragments were synthesized and labeled from 100 ng of total RNA using the GeneChip WT cDNA Synthesis Kit (Ambion, Austin, TX). Hybridization and signal acquisition of the GeneChip Mouse Exon 1.0 ST exon array (Affymetrix, Santa Clara, CA) were performed according to the instructions provided by the manufacturer. Each array experiment was performed in triplicate. The exon-level and gene-level signal intensities were normalized by the RMA and iterPLIER methods, respectively, using the Expression Console 1.1.2 (Affymetrix). We followed the gene annotation of the ENSEMBL version e!61, which is based on the mouse genome assembly NCBI build 37.1/mm9. All microarray data were registered in the Gene Expression Omnibus with accession number GSE36153 for cortical neurons, GSE42421 for motor neurons, glial cells, and cerebellar neurons.

The principal component analysis of innate gene profiles in each cell type was conducted using the GeneSpring software (Agilent Technologies). For each cell type, the gene-level signal intensities of three controls treated with shCont were compared with those of three samples treated either with shFUS1 or shFUS2, using the Student's t-test. The gene expression profiles for each cell-type were established with or without statistical filtration of the t-test p value ≤ 0.1. We also obtained alternative splicing profiles by filtering the exon-level signal intensities of the probe sets on internal exons with t-test p value ≤ 0.1. Comparison analysis of the profiles was completed using shCont and shFUS1 subsets for each cell-type profile.

RT-PCR for alternative splicing analysis. Total RNA was isolated from cells using RNeasy Mini Kit (Qiagen, Hilden, Germany) followed by treatment with DNaseI (Qiagen). cDNA was synthesized from 1 μg of total RNA with the Oligo-dT primer (Promega, Madison, WI). The primers for each candidate exon were designed using Primer3 software (http://frodo.wi.mit.edu/primer3/input.htm). The sequences of primers are shown in Supplementary Table S4. Semi-quantitative RT-PCR was performed using Ex Taq (Takara Bio Inc, Otsu, Japan) at 25–30 cycles at 98°C for 10 sec, 60°C for 30 sec, and 72°C for 1 min. PCR products was electrophoresed on 15% acrylamide gel and stained with ethidium bromide. The intensity of each band was measured by Multi Gage software (Fujifilm, Tokyo).

Immunoblot. Cells were lysed in TNE buffer containing protease inhibitors for 15 min on ice. The lysates were then cleared by centrifuging the cells at 13,000 g for 15 min at 4°C. Lysates were normalized for total protein (10 μg per lane), separated using a 4%–20% linear gradient SDS-PAGE and electroblotted. For immunoblot, we used anti-FUS antibodies (A300-293A, Bethyl Laboratories, Montgomery, TX and 4H11, Santa Cruz Biotechnology, Santa Cruz, CA), anti-Syntaxin-1A antibody (abcam, Cambridge, MA), anti-RD3 antibody (Millipore, Billerica, MA), anti-RD4 antibody (Millipore), anti-Braf antibody (Thermo Scientific, South Logan, UT), and anti-actin antibody (Sigma, St. Louis, MO).

RNA imunoprecipitation (RIP). Extracts were taken from mouse cerebrum, cerebellum, and spinal cord at E15, normalized for total protein (1.6 mg), and applied for RIP using anti-FUS antibody (A300-293A, Bethyl Laboratories) and RIP-Assay Kit (MBL, Nagoya Japan). Immunoprecipitation using rabbit IgG was used as a control. Semi-quantitative RT-PCR was performed using Ex Taq (Takara Bio Inc, Otsu, Japan) and random primers at 22–25 cycles at 98°C for 10 sec, 60°C for 30 sec, and 72°C for 1 min. Based on the HITS-CLIP analysis information in our previous study, we designed primers for *Mapt* at exon6, *Dlgap1* at exon11, and *Stxbp1* at exon20, respectively. Primers for *Gapdh* and an intergenic region were used as controls.

Bioinformatics analysis. The detail was described in Supplementary experimental procedures.

1. Rothstein, J. D. Current hypotheses for the underlying biology of amyotrophic lateral sclerosis. *Ann Neurol* **65 Suppl 1**, S3–9 (2009).
2. Saxena, S. & Caroni, P. Selective neuronal vulnerability in neurodegenerative diseases: from stressor thresholds to degeneration. *Neuron* **71**, 35–48 (2011).
3. Strong, M. J. & Volkening, K. TDP-43 and FUS/TLS: sending a complex message about messenger RNA in amyotrophic lateral sclerosis? *FEBS J* **278**, 3569–77 (2011).
4. Lagier-Tourenne, C. & Cleveland, D. W. Rethinking ALS: the FUS about TDP-43. *Cell* **136**, 1001–4 (2009).
5. Munoz, D. G. et al. FUS pathology in basophilic inclusion body disease. *Acta Neuropathol* **118**, 617–27 (2009).
6. Neumann, M. et al. A new subtype of frontotemporal lobar degeneration with FUS pathology. *Brain* **132**, 2922–31 (2009).
7. Van Langenhove, T., van der Zee, J. & Van Broeckhoven, C. The molecular basis of the frontotemporal lobar degeneration-amyotrophic lateral sclerosis spectrum. *Ann Med* **44**, 817–28 (2012).
8. Kwiatkowski, T. J., Jr. et al. Mutations in the FUS/TLS gene on chromosome 16 cause familial amyotrophic lateral sclerosis. *Science* **323**, 1205–8 (2009).
9. Vance, C. et al. Mutations in FUS, an RNA processing protein, cause familial amyotrophic lateral sclerosis type 6. *Science* **323**, 1208–11 (2009).
10. Deng, H. X. et al. FUS-immunoreactive inclusions are a common feature in sporadic and non-SOD1 familial amyotrophic lateral sclerosis. *Ann Neurol* **67**, 739–48 (2010).
11. Bosco, D. A. et al. Mutant FUS proteins that cause amyotrophic lateral sclerosis incorporate into stress granules. *Hum Mol Genet* **19**, 4160–75 (2010).
12. Dormann, D. et al. ALS-associated fused in sarcoma (FUS) mutations disrupt Transportin-mediated nuclear import. *EMBO J* **29**, 2841–57 (2010).
13. Ito, D., Seki, M., Tsunoda, Y., Uchiyama, H. & Suzuki, N. Nuclear transport impairment of amyotrophic lateral sclerosis-linked mutations in FUS/TLS. *Ann Neurol* **69**, 152–62 (2011).
14. Kino, Y. et al. Intracellular localization and splicing regulation of FUS/TLS are variably affected by amyotrophic lateral sclerosis-linked mutations. *Nucleic Acids Res* **39**, 2781–98 (2011).
15. Wang, J. W., Brent, J. R., Tomlinson, A., Shneider, N. A. & McCabe, B. D. The ALS-associated proteins FUS and TDP-43 function together to affect Drosophila locomotion and life span. *J Clin Invest* **121**, 4118–26 (2011).
16. Kabashi, E. et al. FUS and TARDBP but not SOD1 interact in genetic models of amyotrophic lateral sclerosis. *PLoS Genet* **7**, e1002214 (2011).
17. Boillee, S. et al. Onset and progression in inherited ALS determined by motor neurons and microglia. *Science* **312**, 1389–92 (2006).
18. Yamanaka, K. et al. Mutant SOD1 in cell types other than motor neurons and oligodendrocytes accelerates onset of disease in ALS mice. *Proc Natl Acad Sci U S A* **105**, 7594–9 (2008).
19. Yamanaka, K. et al. Astrocytes as determinants of disease progression in inherited amyotrophic lateral sclerosis. *Nat Neurosci* **11**, 251–3 (2008).
20. Ishigaki, S. et al. Position-dependent FUS-RNA interactions regulate alternative splicing events and transcriptions. *Sci Rep* **2**, 529 (2012).
21. Huang da, W., Sherman, B. T. & Lempicki, R. A. Systematic and integrative analysis of large gene lists using DAVID bioinformatics resources. *Nat Protoc* **4**, 44–57 (2009).
22. Dennis, G., Jr. et al. DAVID: Database for Annotation, Visualization, and Integrated Discovery. *Genome Biol* **4**, P3 (2003).
23. Licatalosi, D. D. et al. HITS-CLIP yields genome-wide insights into brain alternative RNA processing. *Nature* **456**, 464–9 (2008).
24. Masuda, A. et al. CUGBP1 and MBNL1 preferentially bind to 3' UTRs and facilitate mRNA decay. *Sci Rep* **2**, 209 (2012).
25. Xue, Y. et al. Genome-wide analysis of PTB-RNA interactions reveals a strategy used by the general splicing repressor to modulate exon inclusion or skipping. *Mol Cell* **36**, 996–1006 (2009).
26. Keren, H., Lev-Maor, G. & Ast, G. Alternative splicing and evolution: diversification, exon definition and function. *Nat Rev Genet* **11**, 345–55 (2010).
27. Grabowski, P. Alternative splicing takes shape during neuronal development. *Curr Opin Genet Dev* **21**, 388–94 (2011).
28. Yeo, G., Holste, D., Kreiman, G. & Burge, C. B. Variation in alternative splicing across human tissues. *Genome Biol* **5**, R74 (2004).
29. Clark, T. A. et al. Discovery of tissue-specific exons using comprehensive human exon microarrays. *Genome Biol* **8**, R64 (2007).
30. Geser, F. et al. Evidence of multisystem disorder in whole-brain map of pathological TDP-43 in amyotrophic lateral sclerosis. *Arch Neurol* **65**, 636–41 (2008).
31. Ravits, J. M. & La Spada, A. R. ALS motor phenotype heterogeneity, focality, and spread: deconstructing motor neuron degeneration. *Neurology* **73**, 805–11 (2009).
32. Da Cruz, S. & Cleveland, D. W. Understanding the role of TDP-43 and FUS/TLS in ALS and beyond. *Curr Opin Neurobiol* **21**, 904–19 (2011).
33. Lagier-Tourenne, C. et al. Divergent roles of ALS-linked proteins FUS/TLS and TDP-43 intersect in processing long pre-mRNAs. *Nat Neurosci* **15**, 1488–97 (2012).
34. Rogelj, B. et al. Widespread binding of FUS along nascent RNA regulates alternative splicing in the brain. *Sci Rep* **2**, 603 (2012).
35. Orozco, D. et al. Loss of fused in sarcoma (FUS) promotes pathological Tau splicing. *EMBO Rep* **13**, 759–64 (2012).
36. Yoshida, M. Cellular tau pathology and immunohistochemical study of tau isoforms in sporadic tauopathies. *Neuropathology* **26**, 457–470 (2006).
37. Hong, M. et al. Mutation-specific functional impairments in distinct tau isoforms of hereditary FTDP-17. *Science* **282**, 1914–7 (1998).
38. Saitsu, H. et al. De novo mutations in the gene encoding STXBP1 (MUNC18-1) cause early infantile epileptic encephalopathy. *Nat Genet* **40**, 782–8 (2008).
39. Tian, J. H., Das, S. & Sheng, Z. H. Ca2+-dependent phosphorylation of syntaxin-1A by the death-associated protein (DAP) kinase regulates its interaction with Munc18. *J Biol Chem* **278**, 26265–74 (2003).

40. Verheij, C. *et al.* Characterization and localization of the FMR-1 gene product associated with fragile X syndrome. *Nature* **363**, 722–4 (1993).
41. Campeau, E. *et al.* A versatile viral system for expression and depletion of proteins in mammalian cells. *PLoS One* **4**, e6529 (2009).

Acknowledgements

Author contributions

Y.F., S.I., A.M., T.U. and Y.I. performed the experiments. Y.F., S.I., A.M., H.W., K.O. and G.S. analyzed the data. S.I., M.K., K.O. and G.S. prepared the manuscript. All authors reviewed the manuscript.

Additional information

ORIGINAL ARTICLE

Mutations in *COQ2* in Familial and Sporadic Multiple-System Atrophy

The Multiple-System Atrophy Research Collaboration

ABSTRACT

BACKGROUND

Multiple-system atrophy is an intractable neurodegenerative disease characterized by autonomic failure in addition to various combinations of parkinsonism, cerebellar ataxia, and pyramidal dysfunction. Although multiple-system atrophy is widely considered to be a nongenetic disorder, we previously identified multiplex families with this disease, which indicates the involvement of genetic components.

METHODS

In combination with linkage analysis, we performed whole-genome sequencing of a sample obtained from a member of a multiplex family in whom multiple-system atrophy had been diagnosed on autopsy. We also performed mutational analysis of samples from members of five other multiplex families and from a Japanese series (363 patients and two sets of controls, one of 520 persons and one of 2383 persons), a European series (223 patients and 315 controls), and a North American series (172 patients and 294 controls). On the basis of these analyses, we used a yeast complementation assay and measured enzyme activity of parahydroxybenzoate-polyprenyl transferase. This enzyme is encoded by the gene *COQ2* and is essential for the biosynthesis of coenzyme Q_{10}. Levels of coenzyme Q_{10} in lymphoblastoid cells and brain tissue were measured on high-performance liquid chromatography.

RESULTS

We identified a homozygous mutation (M78V-V343A/M78V-V343A) and compound heterozygous mutations (R337X/V343A) in *COQ2* in two multiplex families. Furthermore, we found that a common variant (V343A) and multiple rare variants in *COQ2*, all of which are functionally impaired, are associated with sporadic multiple-system atrophy. The V343A variant was exclusively observed in the Japanese population.

CONCLUSIONS

Functionally impaired variants of *COQ2* were associated with an increased risk of multiple-system atrophy in multiplex families and patients with sporadic disease, providing evidence of a role of impaired COQ2 activities in the pathogenesis of this disease. (Funded by the Japan Society for the Promotion of Science and others.)

The members of the Multiple-System Atrophy Research Collaboration are listed in the Appendix. Address reprint requests to Dr. Shoji Tsuji, Department of Neurology, University of Tokyo, 7-3-1 Hongo, Bunkyo-ku, Tokyo 113-8655, Japan, or at tsuji@m.u-tokyo.ac.jp.

- 115 -

MULTIPLE-SYSTEM ATROPHY IS A PROgressive neurodegenerative disease that is clinically characterized by autonomic failure in addition to various combinations of parkinsonism, cerebellar ataxia, and pyramidal dysfunction. The term multiple-system atrophy was introduced in 1969 to encompass the disease entities of olivopontocerebellar ataxia, striatonigral degeneration, and the Shy–Drager syndrome, on the basis of neuropathological findings in these disorders.[1] Multiple-system atrophy is characterized by the development of cytoplasmic aggregates of α-synuclein, primarily in oligodendroglia.[2-7] However, the pathogenic mechanisms underlying this disease remain unknown, making it difficult to develop effective therapies.

The disorder is classified into two subtypes: subtype C, characterized predominantly by cerebellar ataxia, and subtype P, characterized predominantly by parkinsonism.[8] Among patients with multiple-system atrophy, subtype C has been reported to be more prevalent than subtype P in the Japanese population (65 to 67% vs. 33 to 35%),[9,10] whereas subtype P has been reported to be more prevalent than subtype C in Europe (63% vs. 34%)[11] and North America (60% vs. 13%, with 27% of cases unclassified).[12] Although multiple-system atrophy has been defined as a nongenetic disorder until recently, several multiplex families with the disease have been described, indicating that strong genetic factors confer susceptibility to the disease.[13-15]

METHODS

PATIENTS AND MULTIPLEX FAMILIES

Patients with multiple-system atrophy were enrolled in the study on the basis of research protocols that were approved by the institutional review board at each participating center. Written informed consent was obtained from all participants.

The diagnosis of multiple-system atrophy was made on the basis of the current consensus criteria for the disease.[8] Four Japanese families (Families 1 through 4, whose members have been described previously[13]) and two additional Japanese families (Family 8 and Family 12) were enrolled in this study (Fig. 1). In Family 1, the parents were first-degree cousins, which is consistent with autosomal recessive inheritance. The clinical features of these families are sum-marized in Table S1 in the Supplementary Appendix, available with the full text of this article at NEJM.org.

Autopsy findings for Participants II-4[13] and II-8 in Family 1 and Participant II-6 in Family 8 showed widespread and abundant cytoplasmic aggregates of α-synuclein, primarily in oligodendroglia, in association with neurodegeneration in striatonigral and olivopontocerebellar structures. These findings confirmed the diagnosis of multiple-system atrophy.

PATIENTS WITH SPORADIC DISEASE AND CONTROLS

As with the multiplex families, the diagnosis of sporadic multiple-system atrophy was made on the basis of the current consensus criteria.[8] A total of 363 patients with multiple-system atrophy and 520 controls were included in the Japanese series, 223 patients and 315 controls in the European series, and 172 patients and 294 controls in the North American series (persons of European or Hispanic descent living in North America) (Text S2 and Table S2 in the Supplementary Appendix). Ancestry was determined by self-report on a multiple-choice questionnaire. We also enrolled an independent series of 2383 Japanese controls.

ASSOCIATION WITH OTHER NEURODEGENERATIVE DISEASES

To determine the specificity of the association between variants in candidate genes and multiple-system atrophy, we enrolled 2728 Japanese patients with Alzheimer's disease, 659 with Parkinson's disease, and 634 with amyotrophic lateral sclerosis (ALS). Their demographic characteristics are provided in Text S2 in the Supplementary Appendix.

LINKAGE ANALYSIS AND WHOLE-GENOME SEQUENCING

We performed parametric and nonparametric linkage analyses using Affymetrix SNP 6.0 arrays and software for linkage analysis.[16,17] The genomic DNA from Participant II-4 in Family 1 was subjected to four runs in an Illumina Genome Analyzer IIx (100-bp-long paired ends). We used BWA software[18] and SAMtools sequence-alignment mapping[19] with the default settings for alignment and variation detection against the human reference genome (National Center for Biotechnology Information build 36 [also known as hg18]).